$\chi^{(2)}$-active sol-gel inorganic-organic nanocomposites

R. Kasemann, S. Brück, H. Schmidt

Institute for New Materials (Germany)

L. Kador

University of Bayreuth (Germany)

1. ABSTRACT

Various compositions of inorganic-organic composites (ormocers and nanocomposites) have been synthesized and used as matrices for NLO push-pull molecules. It has been shown that dielectric properties and electrical conductivity during the sol-gel transition (curing parallel to corona poling) are the most important factors for obtaining high $\chi^{(2)}$ efficiencies. With low conductivity systems, $\chi^{(2)}$ values up to 9.7 pm/v have been obtained.

Keywords: non-linear optics, second harmonic generation, sol-gel, inorganic-organic nanocomposites, ormocers, corona poling.

2. INTRODUCTION

Organic molecules with high polarizibility are widely investigated as starting materials for large NLO effects[1,2] for $\chi^{(2)}$ materials with an interesting application potential. For technical application easy processable and stable polymeric materials as matrix for NLO groupings are of special interest. Macroscopic noncentrosymmetric orientation of polarizable organic molecules is necessary for second order nonlinear optical effects. State of the art is orientation of NLO active dipolar molecules incorporated in a polymer matrix by a strong electrical field at temperatures above its glass transition temperature (T_g)[3]. Relaxation of the dipoles into the thermodynamic equilibrium of random orientation occurs even in the glassy state below T_g and leads to decreasing NLO efficiency with time[4]. There are different possibilities to minimize relaxation effects in poled polymers. Polymers with high T_g matrices like polyimide[5] are of interest, but organic NLO molecules must be stable against applied high poling temperatures. In other approaches slower relaxation is achieved by attachment of NLO molecules to a polymer backbone (side-chain, main-chain polymers)[6] and by crosslinking the polymer matrix during poling[7] at moderate temperatures. Reasonable long-term and thermal stability of the $\chi^{(2)}$ parameter has been achieved with both techniques. Inorganic-organic sol-gel-derived composites open the possibility of being processed at slightly elevated temperatures to high T_g materials by condensation reactions forming an inorganic backbone as well as by polymersation. Especially for inorganic-organic nanocomposites it has been shown that they can be prepared with good optical properties (high transparency, low optical loss, tunable refractive index). They can be micropatterned due to their organic crosslinkable part of their matrix[8].

For this reason, it was investigated how far these basic properties can be used for the incorporation of NLO active organic molecules to prepare materials with SHG (second harmonic generation) properties. Stilbene and azobenzene type NLO molecules were included via guest-host principle in inorganic-organic nanocomposites to compare efficiency of their crosslinked matrix as relaxation hinderance with well-characterized guest-host polymers of PMMA type. It has been already shown that SHG effects can be obtained by using these methods[9], but the obtained values had been rather low. As one of the main obstacles the relatively high conductivity of the sols could be identified. For this reason, the present investigations are focused on the processing of low-conductivity sols for more efficient poling.

3. EXPERIMENTAL

Two basic systems of inorganic-organic nanocomposites were used as matrix materials. Synthesis and properties of the photocurable system (A) based on zirconium propoxide (ZR), methacrylic acid (MA), 3-methacryloxypropyl trimethoxy-silane (MPTS) and an initiator for photopolymerisation (1% 1-hydroxycyclohexylphenylketone) were described in detail

0-8194-1612-6/94/$6.00

elsewhere[10]. The thermally curable system (B) is based on 1 mole 3-glycidyloxypropyl trimethoxysilane (GPTS), 0.4 mole of various bis- or tris-(hydroxyphenyl) compounds (either 2,2-bis-(4-hydroxyphenyl)-propane (BPA), bis-(4-hydroxyphenyl)-sulfone (BPS) or 1,1,1-tris-(4-hydroxyphenyl)-ethane (THPE)) and an initiator for thermal curing (1.5 wt% 1-cyanoguanidine (DICY)). The sols were synthesized by stepwise hydrolysis and condensation of the alkoxide precursors with water in the ratio 1.5 mole water per mole silane. Addition of the hydroxyphenoles was performed after 24 h catalyst-free hydrolysis of the silane at 100 °C or after 4 h acid-catalyzed (0.1n HCl) hydrolysis at room temperature. Hydrolysis, condensation, water content, silanole concentration and conductivity were followed with Karl-Fischer titration, IR, ^{29}Si-NMR spectroscopy and measurements with a conductivity meter LF 196 (from WTW, Germany). Guest-host type chromophores 4-(N,N-dimethylamino)-4'-nitrostilbene (DANS) or Disperse Red 1 (DR1) were added as saturated tetrahydrofurane solution. The dye content in the films was determined with UV/Vis spectroscopy. Side-chain type bonded modified NLO chromophore N-[3-(triethoxysilyl)propyl]-2,4-dinitrophenylamine (TDP) was 24 h cohydrolyzed and cocondensated in hydrolyzed GPTS/BPA solution. After addition of the curing initiator the viscous sols were deposited by spin-coating on indium-tin-oxide (ITO) coated glass slides. The samples were subjected to positive voltage (8 kV) corona poling in a geometry with two 50 µm diameter gold wires positioned about 15 mm above the film. During poling the sol-gel transformation in both systems was initiated by heating up to 130°C. Additional 10 min UV light illumination with a 200 W Hg lamp was applied in system A. The basics of the preparation are shown in fig. 1.

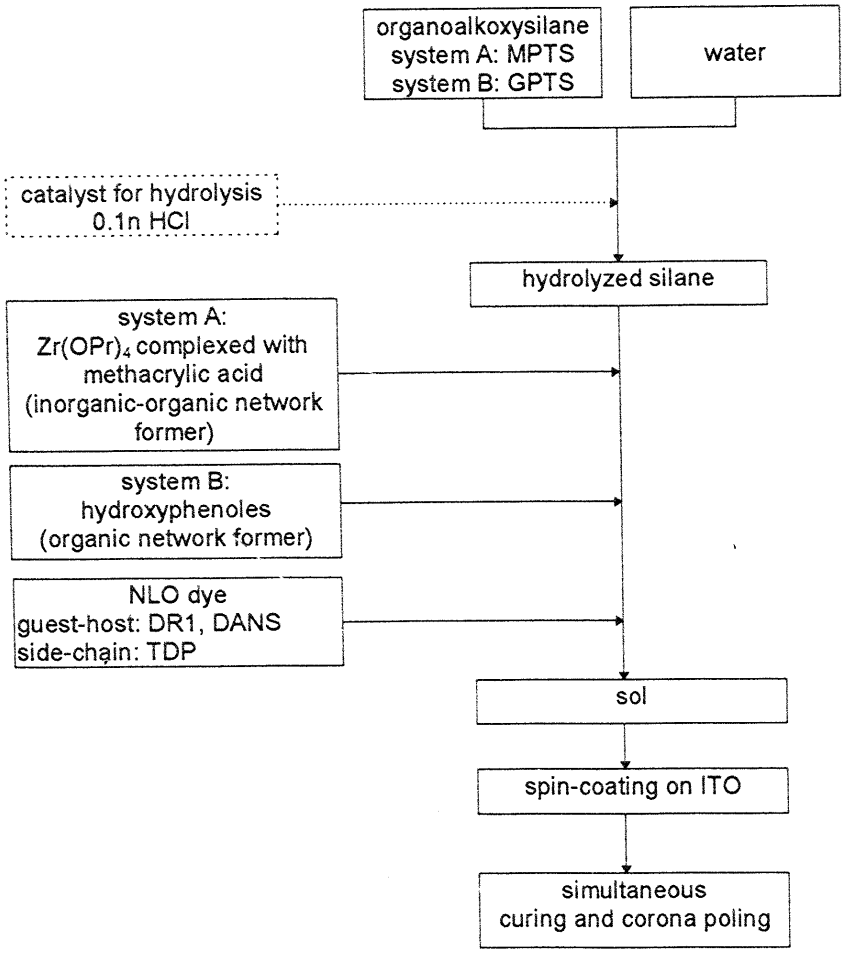

Fig. 1: Flowchart of the preparation of NLO active inorganic-organic nanocomposites A and B.

Dielectric measurements during curing process were performed between two ITO coated glass slides electrically connected to a Zahner impedance analyzer. Both impedance and phase shift were monitored versus temperature and time. In situ measurements of developing SHG activity by orientation during poling and curing of system B are performed with a

heatable corona poling cell in a transmission setup. Temperature range and time scale of all experiments were described in the following results and discussion section. For time-dependent measurements of $\chi^{(2)}$ values with the Maker fringe technique[11] simultaneously during the poling and curing process the in situ SHG and poling device (fig.5) is mounted on a rotation stage.

4. RESULTS AND DISCUSSION

Transparent material A was chosen as a model for the guest-host type matrix for DR 1. Sols from system A are photo-curable due to methacrylic groupings from MPTS as well as from MA. Gel formation is obtained by a two-step process with heat and UV light, which opens the additional possibilities to produce waveguide structures in a laser writing process, as already shown in[10]. Film preparation and the used measurement technique has been published in detail[9]. Measurements of SHG signal up to five months after poling and curing process are performed to obtain information about the long-term stability (fig. 2).

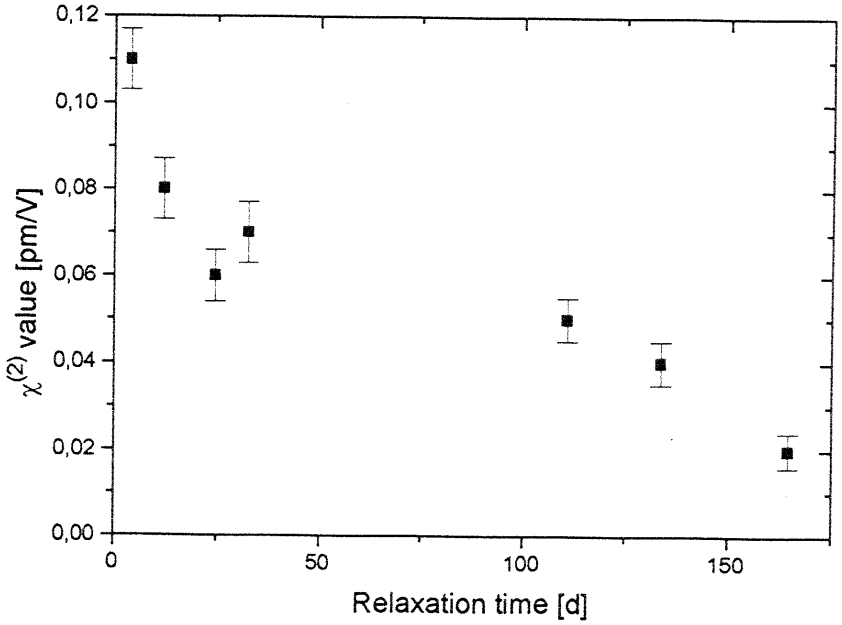

Fig. 2: Relaxation of 5 wt.% DR1 in corona poled system A (MPTS/ZR/MA)

The SHG coefficient decreases by a factor of roughly 6 after five months. Thus the stability is still better than that of PMMA matrices doped with physically dissolved dye molecules[12] which can be interpreted by the rigidity of the matrix. However, the overall magnitude of the $\chi^{(2)}$ parameter of 0.1 pm/V is rather small. The $\chi^{(2)}$ parameter for one given NLO dye is dependent on concentration and orientation degree of dye molecules. Since concentration of NLO molecules in the matrix is with 5 wt.% as high as in PMMA matrices, the low $\chi^{(2)}$ values only can be attributed to a low orientation efficiency. For this reason, the electrical conductivity has been measured. With 54 µS/cm it is very high, and the transport of corona-generated ions from the film surface reduces the effective poling field and poling efficiency. One source of ionic conductivity was found to be the formation of zirconates from hydrolyzed zirconium propoxide, used as catalyst for condensation of hydrolyzed silane species. Monitoring the electrical conductivity, it was found that it increases from 2 µS/cm to 54 µS/cm after the zirconate formation. One other source of conductivity is the addition of hydrochloric acid necessary as a catalyst for hydrolysis of GTPS or MPTS and its incomplete removal.

In order to minimize the conductivity, an alternative route was developed for the hydrolysis of organoalkoxysilanes employing elevated temperatures of 100 °C without any catalyst. Hydrolysis rates of GTPS with 0.1n HCl as a catalyst and without any catalyst at two different temperatures are determined by Karl-Fischer titrations, shown in figure 3.

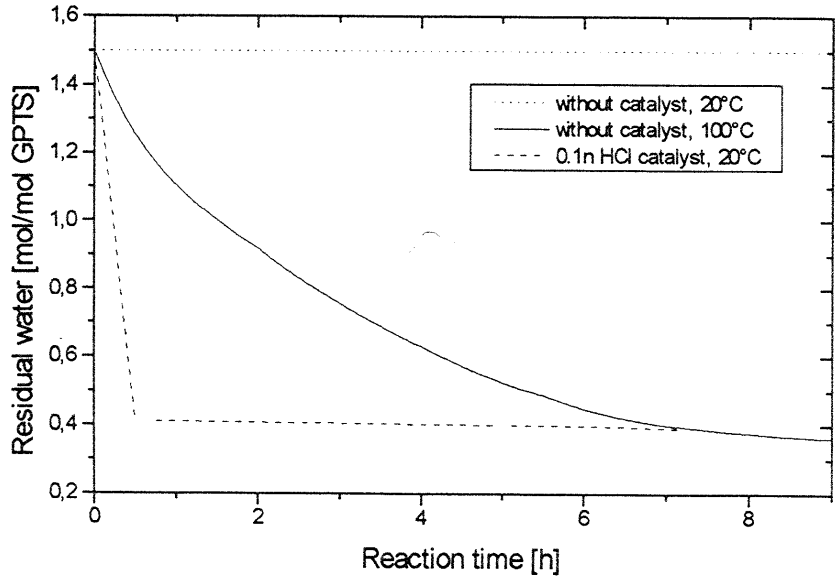

Fig. 3: Water content with reaction time during the GPTS hydrolysis.
(Karl-Fischer titration, initial GPTS:water ratio = 1:1.5 mole)

Hydrolysis times up to 9 h of GPTS at 100 °C without catalysts are necessary in order to get a hydrolysis extent comparable to an acid catalyzed reaction path at room temperature (fast hydrolysis within 0.5 h at room temperature). The residual water contents and the silanole/silixane contents (measured by ^{29}Si-NMR) of the acid free hydrolysis (9 h) and the o.1n HCl hydrolysis (0.5 h) are similar. The hydrolyzed solutions with acid catalyst show a conductivity of 0.7 µS/cm due to mobile protons whereas the acid-free hydrolyzed solutions have a low conductivity of 0.3 µS/cm. Hydroxyphenyl compounds (BPA, BPS or THPE) are added to the hydrolyzed GPTS sols according to fig. 1. The resulting ionic conductivity of 0.3 µS/cm is several magnitudes lower than in system A and lower than in system B with acid catalysis. Formation of an organic network occurs by polyaddition reactions with GPTS after addition of a starter (DICY) and thermal treatment. Analogous guest-host incorporation of DANS or DR1 in system B sols leads to various materials with significant higher $\chi^{(2)}$ values than in system A (see table 1), attributed to the decreased conductivity and thereby increased field strength during corona poling.

Table 1: Influence of the precuring of the inorganic network before corona poling on achieved $\chi^{(2)}$ values. (Precuring step: 1 h 70 °C, Curing and corona poling step: ~7 kV at 130 °C for 1 h).

System	Guest-Host molecule	$\chi^{(2)}$ value after poling without precuring [pm/V]	$\chi^{(2)}$ value after poling with precuring [pm/V]
GPTS:BPA	0.5 wt% DANS	0.0	0.3
GPTS:BPS	0.5 wt% DANS	0.5	0.8
GPTS:BPA	1.5 wt% DR 1	0.5	9.7

The observed $\chi^{(2)}$ values are dependent on the applied curing and poling process. The additional precuring of samples (1 h at 70 °C) results in better SHG efficiency. With DANS the difference of 0.3 pm/V between the two curing processes is independent of organic network former BPA or BPS. It is assumed that curing of the inorganic network takes place in the precuring step because the formation of organic networks requires higher temperatures. Network formation itself has a significant influence on the mobility of charge carriers. Additionally water, methanol and silanol (generated by hydrolysis of alkoxysilanes) concentrations are decreased by evaporation and polycondensation at elevated temperatures. In order to monitor these changes in charge carrier mobility and concentration time-dependent dielectric measurements during the curing process are performed. In figure 4 resistance and phase shift of a dielectric layer of a system B sol is shown depending on the curing time.

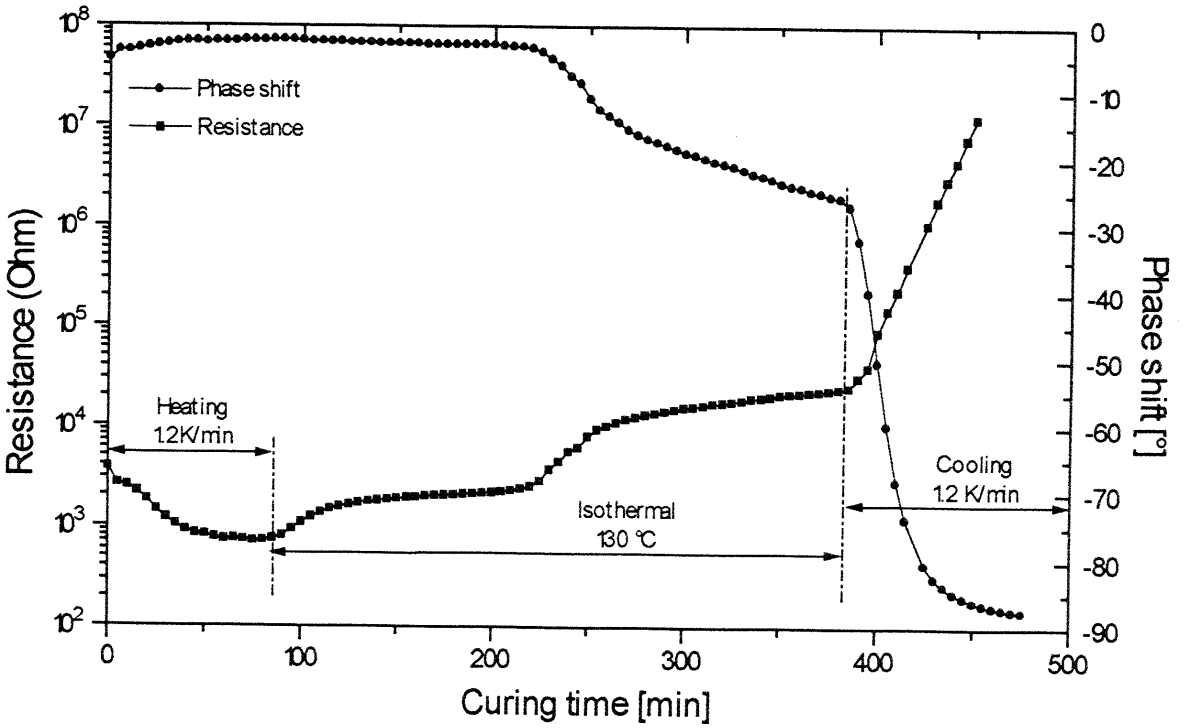

Fig. 4: Dielectric measurements of impedance and phase shift during cure of GPTS/BPA/THPE sol with DICY as curing agent (GPTS:BPA:THPE = 1:0.2:0.13 mole, Frequency 1kHz).

In the heating step observed resistance decreases when ionic mobility increases with temperature. In the isothermal step the observed resistance is increased when viscosity increases through gel formation, evaporation of water and methanol and condensation of weak acid silanoles to siloxanes. The phase shift is only about -3° in the first 220 min of the curing process. This is almost a resistor characteristic of Ohm type and not an insulator as required for an efficient poling. After 220 min a second resistance reducing process starts. This can be explained by the formation of the organic network. The material develops slowly insulator properties and phase shift decreases down to -25° (perfect insulator = capacitor: -90 °). In the cooling step resistance increases several magnitudes when ion mobility is reduced. The final material is a capacitor with phase shift of about -88° Corona poling depends on existence of an insulator layer where charges are deposited and form an electrical field against a counter electrode. The measurements show that these properties are achieved in the last steps of the curing process when organic crosslinking takes place and when the material is cooled down from curing temperature.

In order to be able to correlate the dielectric and the conductivity data to poling efficiency, a device was developed to monitor the SHG signal during the poling and curing process (fig. 5).

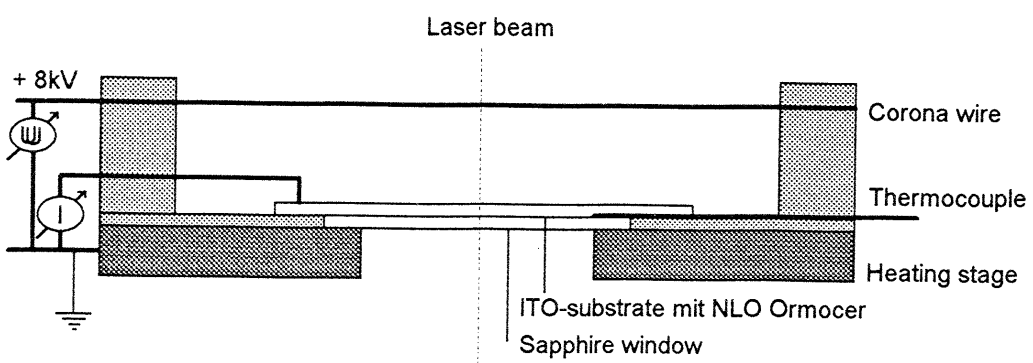

Fig. 5: Schematic of the in-situ-poling and SHG monitoring device.
The device is mounted of a rotaion stage for Maker fringe[11] measurements.

Figure 6 shows the time-dependent SHG signal during the cooling step of curing and poling process. In this sample GPTS/BPA is modified with side-chain type incorporated N-[3-(triethoxysilyl)propyl]-2,4-dinitrophenylamine (TDP). TDP is a well-characterized NLO molecule and was incorporated successfully in inorganic sol-gel matrices[13,14]. The yellow dye does not have any absorbence at the second harmonic wavelength of 532 nm and measured SHG signals are not enhanced by any resonance (like in the red dyes DANS and DR1).

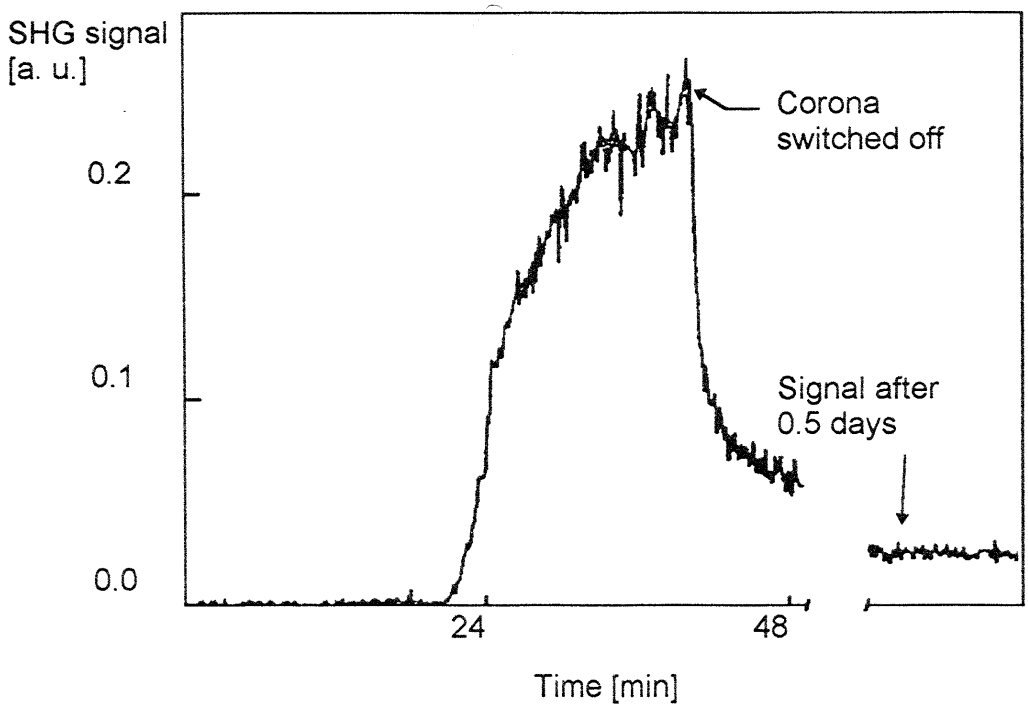

Fig. 6: *In situ* measurement of SHG activity at 1064 nm wavelength during poling of GPTS/BPA/TDP. The sample is in the cooling stage after 3 h isothermal curing at 130 °C (see fig. 4).

In the heating step and in the isothermal step no detectable SHG signal is generated in the sample. Ionic conductivity is still too high to allow formation of the charged layer on the sample. SHG starts in the cooling step when the temperature of the material is below 60 °C and the signal increases with decreasing temperature. The signal decreases strongly after switching off the corona voltage (40 min). Several hours later a stable signal of about 10% of the maximum value with applied corona field is measured. This value is comparable with samples with conventional curing and poling (without *in situ* monitoring) up to 2.6 pm/V. The SHG signal is proportional to the square of the $\chi^{(2)}$ parameter[15] and a transient signal of 8 pm/V is estimated.

5. Conclusions

The investigations have shown that ionic conductivity and dielectric properties of the matrix are the key for obtaining high $\chi^{(2)}$ values. The results show that by adapting all synthesis and processing parameters in combination with dielectric and in situ $\chi^{(2)}$ measurements simultaneous to poling and curing, an optimization strategy can be developed, which will be used for investigations for further enhancement of $\chi^{(2)}$ efficiency and long-term stability.

6. Acknowledgments

The financial support of the Volkswagen-Stiftung (Germany) is gratefully acknowledged.

7. References

1. D. J. Williams, Angew. Chem. Intl. Ed. Eng. **23**, pp. 690, 1984.
2. J. Zyss, J. Molec. Electron. **1**, pp. 25, 1985.
3. G. R. Meredith, J. van Dusen, D. J. Williams, Macromolecules **15**, pp. 1385, 1982.
4. K. D. Singer *et. al.*, Appl. Phys. Lett. **49**, pp. 248, 1986.
5. J. W. Wu *et. al.*, Appl. Phys. Lett. **51**, pp. 225, 1991.
6. H. T. Man, K. Chiang, D. Haas, C. C. Teng, H. N. Yoon, SPIE **1213**, pp. 7, 1990.
7. M. Eich, B. Reck, D. Y. Yoon, C. G. Wilson, G. C. Bjorklund, J. Appl. Phys. **66** , pp. 3241 1989.
8. H. Schmidt, M. Popall, SPIE **1328**, pp. 249, 1990.
9. L. Kador, R. Fischer, D. Haarer, R. Kasemann, S. Brück, H. Schmidt, H. Dürr, Adv. Mater. **4**, pp. 270, 1993.
10. P. D. Maker, R. W. Terhune, M. Niesenoff, C. M. Savage, Phys. Rev. Lett. **8**, pp. 21, 1962.
11. H. Schmidt, H. Krug, R. Kasemann, N Merl, V. Gerhard, F. Tiefensee, S. Brück, in: Hommage to Galileo (Ed: P. Mazzoldi), p. 303, CLEUP, Padova, 1992
12. K. D. Singer, L. A. King, J. Appl. Phys. **70**, pp. 3251, 1991.
13. E. Toussaere, J. Zyss, P. Griesmar, C. Sanchez, Nonlinear Optics **1**, pp. 349, 1991.
14. J. Kim, J. L. Plawsky, R. La Peruta, G.M. Korenowski, Chem. Mater. **4**, pp. 249, 1992.
15. J. Jerphagnon, S. K. Kurtz, J. Appl. Phys. **41**, pp. 1667, 1970.